Korean Journal of Geomatics
Vol. 5, No. 1 / December 2005
pp. 7~19

Invited Paper

Photogrammetric Georeferencing Using LIDAR Linear and Areal Features

Ayman HABIB*, Mwafag GHANMA* and Edson MITISHITA**

Abstract

Photogrammetric mapping procedures have gone through major developments due to significant improvements in its underlying technologies. The availability of GPS/INS systems greatly assist in direct geo-referencing of the acquired imagery. Still, photogrammetric datasets taken without the aid of positioning and navigation systems need control information for the purpose of surface reconstruction. Point features were, and still are, the primary source of control for the photogrammetric triangulation although other higher-order features are available and can be used. LIDAR systems supply dense geometric surface information in the form of three dimensional coordinates with respect to certain reference system. Considering the accuracy improvement of LIDAR systems in the recent years, LIDAR data is considered a viable supply of photogrammetric control. To exploit LIDAR data, new challenges are poised concerning the representation and reference system by which both the photogrammetric and LIDAR datasets are described. In this paper, registration methodologies will be devised for the purpose of integrating the LIDAR data into the photogrammetric triangulation. Such registration methodologies have to deal with three issues: registration primitives, transformation parameters, and similarity measures. Two methodologies will be introduced that utilize straight-line and areal features derived from both datasets as the registration primitives. The first methodology directly incorporates the LIDAR lines as control information in the photogrammetric triangulation, while in the second methodology, LIDAR patches are used to produce and align the photogrammetric model. Also, camera self-calibration experiments were conducted on simulated and real data to test the feasibility of using LIDAR patches for this purpose.

Keywords : *Registration, LIDAR, photogrammetry, triangulation, linear features, areal features, self-calibration*

1. Introduction

The advent of LIDAR data acquisition systems offered the possibility of rapid terrestrial and aerial mapping. Systems that can measure several thousand points per second allow a spatial density distribution of observed coordinates far in excess of that available with traditional surveying and photogrammetric techniques. Such a large sample size can provide a wealth of information for many applications such as surface reconstruction, structural monitoring, orthophoto generation, city mapping, etc. (Lichti et al. 2000). Using LIDAR, there is no inherent redundancy in the computation of the reconstructed surface. Therefore, the overall accuracy depends on the accuracy and calibration of different components comprising the LIDAR system. The positional nature of LIDAR data collection makes it difficult to derive semantic information from the captured surfaces - e.g., material and types of observed structures, even with the presence of intensity images (Wehr and Lohr 1999, Baltsavias 1999, Schenk 1999).

Reconstructed surfaces using photogrammetric techniques, on the other hand, are rich with semantic information that can be easily identified in captured imagery. In addition to that, such surfaces tend to be highly accurate due to the inherent redundancy associated with photogrammetric intersection. Surface reconstruction using metric cameras is a well established methodology that has been repeatedly tested and proven over time. Still, photogrammetric reconstruction of real surfaces requires enough control information to re-establish the position and orientation of imagery (Kraus 1993). Such control can be in the form of

*Department of Geomatics Engineering, University of Calgary, 2500 University Drive NW, Calgary, Alberta, T2N 1N4, Canada, (E-mail : habib@geomatics.ucalgary.ca)
**Department of Geomatics, Federal University of Parana, UFPR, Curitiba, Parana, Brazil (E-mail : mitishita@ufpr.br)

The manuscript for this paper was accepted on October 7, 2005

indirect geo-referencing through ground control points/ features, or in the form of direct geo-referencing through GPS/INS systems on the imaging platform (Mikhail et al. 2001). The drawback of surface reconstruction from imagery is the significant time consumed by the process of manually identifying conjugate points in overlapping images. Automating the matching problem is a difficult task, especially when dealing with large scale imagery over urban areas (Schenk and Csatho 2002).

The complementary nature of LIDAR and photogrammetric data is continuously pushing towards the integration of both systems. Such integration would lead to a more complete surface description from semantic and geometric points of view (Baltsavias 1999, Satale and Kulkarni 2003). The quality of the final synergic product unquestionably depends on the quality achieved from each individual system. Hence, a precise calibration of both systems, which is separately implemented for each system, would guarantee that both datasets are free of systematic errors (Schenk et al. 2001). In addition to the calibration requirement for both systems, the synergic characteristics of both systems can be fully utilized only after successful registration of the datasets relative to a common reference frame (Habib and Schenk 1999). The variation of reference frames between LIDAR and photogrammetric datasets can occur for several reasons. For example, in many cases, photogrammetric and LIDAR data collection missions are launched and processed independently of each other; hence, the reference frames might vary accordingly. Furthermore, previously processed and archived photogrammetric datasets might be utilized with more recent photogrammetric and LIDAR datasets for change detection purposes; again, there is no guarantee that all reference frames will be similar. As another example, imaging sensors might be flown on the same platform as the LIDAR without being bore-sighted relative to the onboard GPS/INS units. In this case, the processing of image data will depend on visible control, which might be in a different reference frame than that of the LIDAR's. A deceptive source of variation in reference frames can be the re-definition of the same reference frame over different periods of time. The same generic name of such a re-defined reference frame can lead to the false belief of identical reference frames.

From the above discussions of photogrammetric and LIDAR geo-referencing, it can be inferred that datasets from both sources are not necessarily in the same reference frame. Considering the vast heritage of existing LIDAR and photogrammetric datasets and the ones being acquired, the importance of a proper co-registration methodology is obvious and indispensable. The majority of registration methodologies rely on point primitives for solving the registration problem between two datasets. Such methodologies are not applicable to LIDAR surfaces since they correspond to laser footprints instead of distinct points that could be identified in the imagery (Baltsavias, 1999). Conventionally, surface-to-surface registration and comparison have been achieved by interpolating both datasets into a uniform grid. The comparison is then reduced to estimating the necessary shifts by analyzing the elevation differences at corresponding grid posts (Ebner and Ohlhof 1994; Kilian et al. 1996). This approach has several limitations. Firstly, the interpolation to a grid will introduce errors especially when dealing with captured surfaces over urban areas. Secondly, minimizing the differences between surfaces along the Z direction is only valid when dealing with horizontal planar surfaces (Habib and Schenk 1999). Postolov et al. (1999) presented another approach, which works on the original scattered data without prior interpolation. However, the implementation procedure involves an interpolation of one surface at the location of conjugate points on the other surface. Additionally, the registration is based on minimizing the differences between the two surfaces along the Z direction. Schenk (1999) introduced an alternative approach where distances between points of one surface along surface normals to locally interpolated patches of the other surface are minimized. Habib et al. (2001) implemented this methodology within a comprehensive automatic registration procedure. This procedure is based on processing the photogrammetric data to produce object-space planar patches. A common problem in the above techniques is that they are 3-D to 3-D registration methodologies, i.e. the photogrammetric model should be established first. However, a 2-D to 3-D registration is needed to relate 2-D imagery to 3-D LIDAR data.

This paper introduces two approaches for the co-registration of LIDAR and photogrammetric surfaces relative to a common reference frame. The registration is achieved through the use of linear and areal features derived from LIDAR data as control information. The following three sections address the general methodologies and mathematical models of the suggested approaches. Section 5 outlines the experimental results from simulated and real datasets captured by LIDAR and metric camera. Finally, Section 6 highlights the research conclusions and recommendations for future work.

2. The Co-registration of Photogrammetric and LIDAR Datasets - Overview

In general, the main purpose of a registration procedure is to combine two or more datasets acquired by the same or different sensors for the purpose of achieving enhanced accuracy and improved inference about the environment than could be attained through the use of one dataset. For this purpose, a registration methodology must consider three essential components: the choice of primitives, the registration transformation parameters of a mathematical model that relates the reference frames under consideration, and finally, the similarity measures that ensure the coincidence of conjugate primitives after applying the appropriate transformation (Brown 1992). In the sub-sections below, a general idea of the basic components of the registration process is presented followed by the co-registration methodologies of photogrammetric and LIDAR datasets.

2.1 Selecting the Registration Primitives

Common features within all datasets should be identified and extracted to be used in relating the datasets in question. The implementation of subsequent registration steps is greatly influenced by the type and representation of the selected primitives. Hence, it is important to decide upon the appropriate primitives to be used for establishing the transformation between the datasets under consideration (Habib and Schenk 1999). In the following paragraphs, the types of candidate primitives are discussed while the representation issue is explained within the context of the respective methodologies.

The three fundamental and most commonly used registration primitives are points, lines, and areal regions (refer to Figure 1 for examples of such primitives in imagery). Candidate features include road intersections, corners of buildings, rivers, coastlines, roads, lakes, and similar dominant man-made or natural structures.

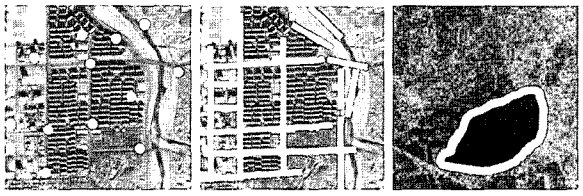

Fig. 1. Examples of primitive alternatives in imagery.

In the registration procedures where point primitives are used, it is almost straightforward to measure points on the set of imagery whereas it is nearly impossible to link the laser footprint with the corresponding image point due to the random nature of LIDAR point collection. However, at a higher processing cost, three intersecting LIDAR patches can be segmented and utilized to extract points, which can then be identified in the imagery. The above obstacles exclude point primitives from being appropriate registration primitives. As a result, linear and areal features are the other potential primitives that can be more suitable for datasets involving LIDAR data. For these primitives, the geometric distribution of individual points makes up the feature rather than individual occurrences, Figure 2. Linear features can be directly measured in overlapping imagery. Conjugate LIDAR lines can be extracted through the use of homogeneous patch segmentation followed by intersection techniques, Figure 3a. Alternatively, LIDAR lines can be directly identified in the intensity images produced by most of today's LIDAR systems, Figure 3b.

Areal primitives (e.g., lakes, roofs, and homogeneous regions) can be extracted from LIDAR datasets using classification or segmentation algorithms. The richness of urban areas with well-defined geometric shapes like roofs makes it possible to collect photogrammetric areal features represented by distinct points along the

Fig. 2. Lines and areas as clusters of individually measured points.

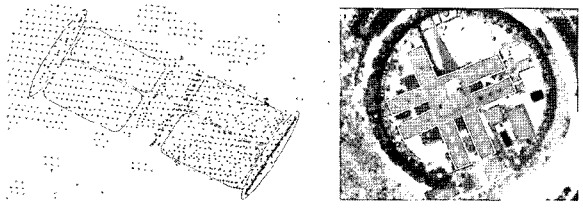

Fig. 3. LIDAR lines from intersecting planar patches (a) and as measured from intensity image (b).

boundaries of such features. In conclusion, linear and areal features will be tested for their suitability and efficiency to perform the registration between the LIDAR and photogrammetric datasets.

2.2 Transformation Function and Similarity Measure

The most fundamental problem of any registration technique is the type of spatial transformation or mapping function needed to properly overlay the two datasets. Based on the application scope, a transformation function might be global or local. A global transformation involves a single set of equations which optimally registers the entirety of the involved datasets. On the other hand, local transformation functions utilize several sets of equations by partitioning the area of interest into regions with each one having its own transformation. In general, local transformations are more accurate but also more computationally demanding.

The role of similarity measure is to introduce the necessary constraints for ensuring the coincidence of conjugate photogrammetric and LIDAR primitives after applying the proper transformation function. The formulation of the similarity measure depends on the selected registration primitives and their respective attributes (i.e., representation scheme). In addition, the similarity measure depends on the utilized methodology for incorporating the LIDAR and photogrammetric data in the registration process.

To explain the two components above, an example of registering a photogrammetric and a LIDAR datasets with conjugate point features will be used. It is important to mention that in the absence of systematic errors, the registration of the datasets is actually a transformation and alignment between the reference frames in which the datasets are described. In this example, the registration can be carried out using one of two alternative methodologies. The first method incorporates LIDAR points directly into the photogrammetric bundle adjustment as control points. Here, the collinearity model is used to project the 3-D LIDAR points into the 2-D image space. This projection includes scale, translation, and rotation parameters that are applied to the LIDAR points. The similarity measure is implicitly considered by constraining the difference between the 2-D location of the measured image point and the 2-D location of the projected LIDAR point to be zero plus or minus the effect of the random noise in the involved measurements.

In the second scenario, a 3-D photogrammetric model is computed first using an arbitrary reference frame without the need for any ground control points. Then, a 3 D similarity transformation is used to scale, shift, and rotate this model from the arbitrary reference frame to that of the LIDAR's. The similarity measure in this case is that the 3-D spatial distance between the photogrammetric model points after being transformed and their conjugates in LIDAR dataset must be zero. In analogy to what is mentioned in this example, specific transformation models and similarity measures should be devised for straight-line and planar-patch features.

3. Registration Methodology Using Linear Features

Linear features can be considered as suitable primitives for the following reasons:

- Compared to distinct points, linear features have higher semantics, which can be useful for subsequent processes (such as DEM generation, map compilation, change detection, and object recognition).
- It is easier to automatically extract linear features from different-type and different-resolution datasets rather than distinct points. This can be attributed to the nature of linear features, since they represent discontinuities in one direction. On the other hand, point features represent discontinuities in all directions.
- Datasets over man-made environments are rich with linear features.
- Linear features can be extracted with adequate accuracy across the direction of the edge.
- Linear features allow for the incorporation of areal features through the use of their boundaries.

Linear features include those described by an analytical function (e.g., straight lines, conic sections, or parametric functions) or by a free form shape (Habib et al. 2002a). In this research, straight-line segments have been chosen as the registration primitives for the following reasons:

- Man-made environments are rich with straight lines.
- Straight lines are easier to detect in different datasets, and the correspondence problem between conjugate features becomes easier to solve.
- Straight-line parameters can be accurately derived from the involved datasets.
- It is straightforward to develop mathematical constraints (similarity measures) describing the correspondence of conjugate straight-line segments.
- Free-form linear features can be represented with

sufficient accuracy as a sequence of straight-line segments (polylines).

For straight-line segments as the registration primitives, one must decide on the representation and extraction methodologies from LIDAR and photogrammetric datasets. These issues will be discussed in the following subsections.

3.1 LIDAR and Photogrammetric Straight-Line Features

In the approach of using line segments as the registration primitives, LIDAR lines will be used as the source of the required control to align the photogrammetric model relative to the LIDAR reference frame. In this regard, one should note that the datum for the LIDAR data is established by the combination of high-quality GPS/INS units onboard the sensor platform. To devise a practical scheme by which straight lines can be extracted from the photogrammetric datasets, the representation of such straight lines in the object and image space must be clearly stated and justified. As detailed in Habib et al. 2002b, the most convenient representation of object space straight lines from a photogrammetric point of view is using two points along the line since it yields well-defined line segments. For this reason, LIDAR lines will be represented by the coordinates of its end points, Figure 4 (a). On the other hand, image space lines will be represented by a sequence of 2-D coordinates of intermediate points along the feature, Figure 4 (b). This is an appealing representation since it can handle

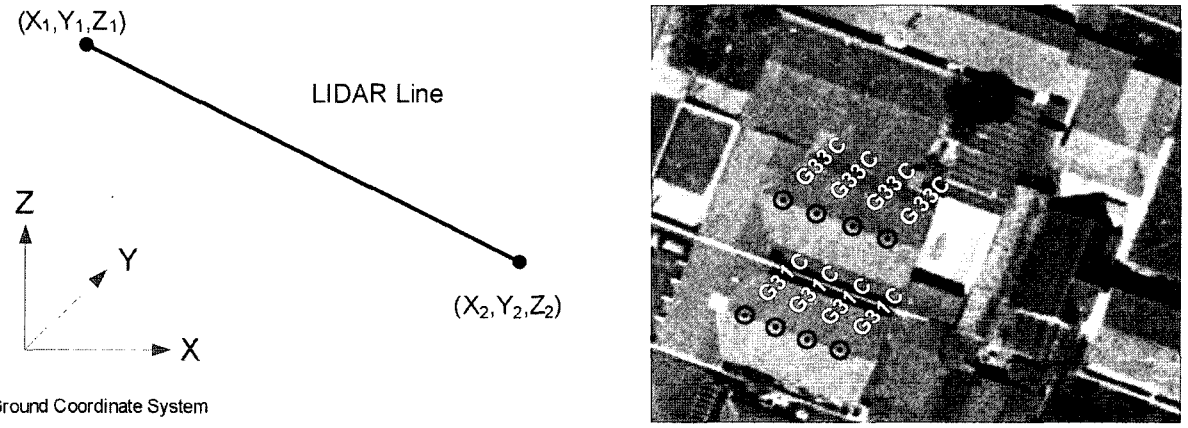

(a) (b)

Fig. 4. LIDAR lines represented by its 3-D end points (a) and image lines measured as a sequence of 2-D intermediate points (b).

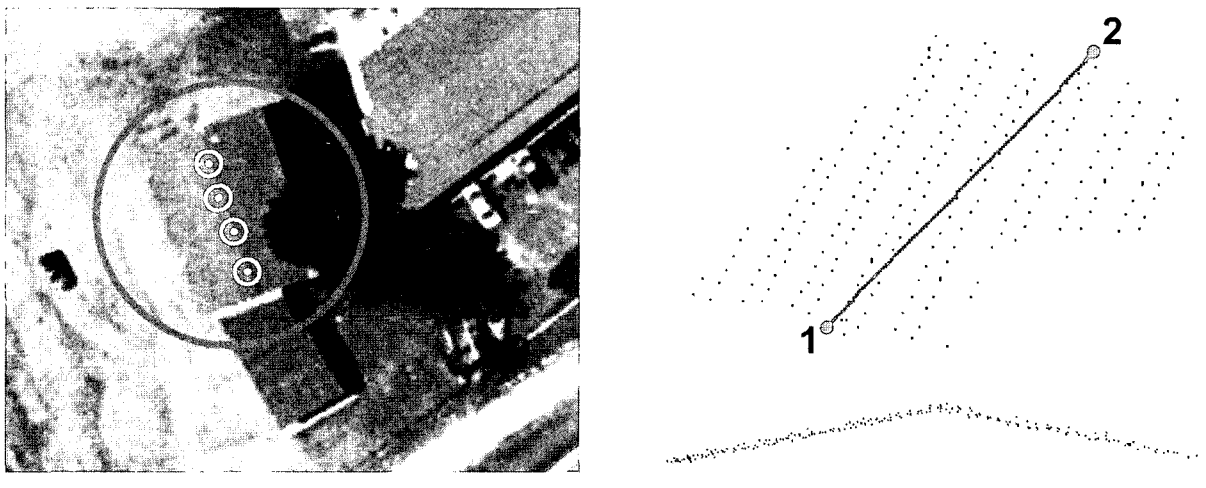

(a) (b)

Fig. 5. Manually identified photogrammetric line (a) and its conjugate in LIDAR data (shown in side and perspective views) (b) as derived from the intersection of neighboring planar patches.

image space linear features in the presence of distortions as they will cause deviations from straightness. Furthermore, it will allow for the inclusion of linear features in scenes captured by line cameras since the imaging process of such cameras leads to deviations from straightness in image space linear features, which correspond to object space straight lines (Habib et al. 2002b). It is important to emphasize that no point-to-point correspondence is needed along conjugate LIDAR and photogrammetric lines.

There are different approaches by which LIDAR lines can be collected. In this work, LIDAR lines are extracted from the intersection of neighboring planar patches. First, suspected planar patches in the LIDAR dataset are manually identified with the help of corresponding optical imagery, Figure 5. The selected patches are then checked using least-squares adjustment to determine whether they are planar or not and to remove blunders. Finally, neighboring planar patches with different orientation are intersected to determine the end points along object space linear features between the patches under consideration. It is important to note that automatic extraction of straight lines is beyond the objectives of this study and will be investigated in future work. Moreover, the correspondence between linear features in photogrammetric and LIDAR datasets is established manually. Following the extraction of straight-lines from both datasets, the focus will be shifted towards selecting proper transformation function and similarity measures that can faithfully represent the transformation and coincidence of conjugate primitives in the involved datasets.

3.2 Transformation Function and Similarity Measure

In this research, the photogrammetric dataset will be aligned to the LIDAR reference frame through direct incorporation of LIDAR lines as the source of control in the photogrammetric bundle adjustment. This procedure will incur that the LIDAR lines will be projected onto the image space through translation, rotation, and scale. The similarity measure mathematically ensures that the projected LIDAR lines on the image space coincide with the corresponding image lines. Here, the transformation function and similarity measure are both implemented simultaneously in a coplanarity condition as shown in Figure 6. This constraint, which is applied for each intermediate point, indicates that the vector from the perspective centre to any intermediate image point along the line is contained within the plane defined by the perspective centre of that image and the two points defining the

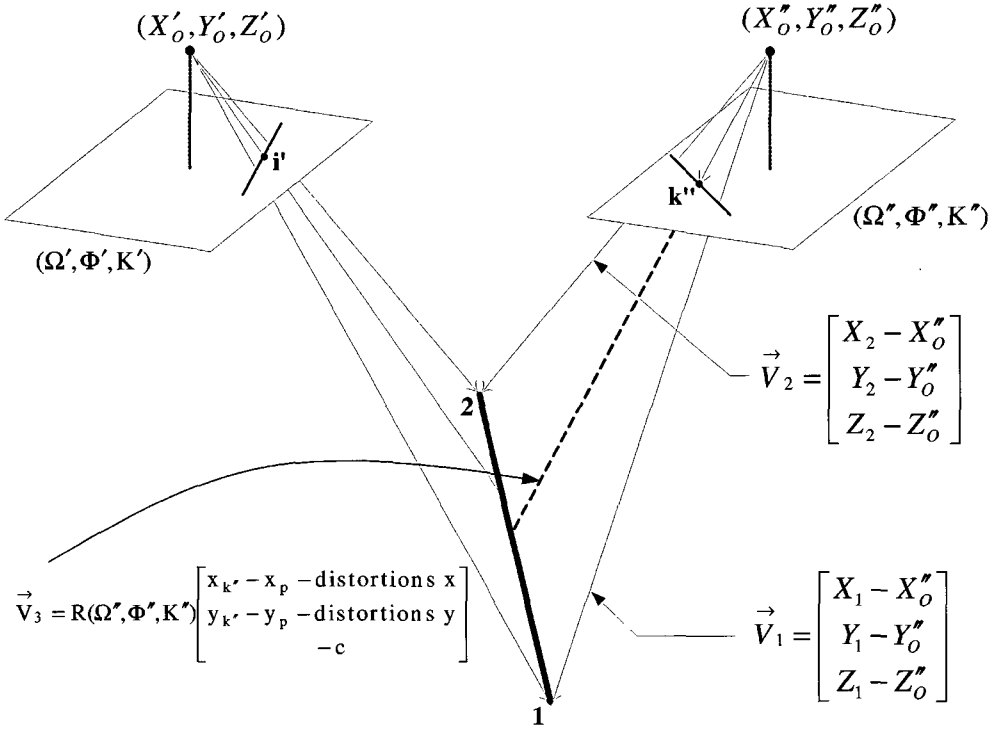

Fig. 6. Perspective transformation between image and LIDAR straight lines and the coplanarity constraint for intermediate points along the line.

LIDAR line. In other words, for a given intermediate point, k'', the points $\{(X_1, Y_1, Z_1), (X_2, Y_2, Z_2), (X_O'', Y_O'', Z_O'')$, and $(x_{k''}, y_{k''}, 0)\}$ are coplanar. This coplanarity constraint is mathematically represented in Equation 1.

$$(\overrightarrow{V_1} \times \overrightarrow{V_2}) \cdot \overrightarrow{V_3} = 0 \quad (1)$$

Where V_1 is the vector connecting the perspective centre to the first end point along the LIDAR line, V_2 is the vector connecting the perspective centre to the second end point along the LIDAR line, and V_3 is the vector connecting the perspective centre to an intermediate point along the corresponding image line.

One should note that this condition assumes that LIDAR data is free from any systematic errors which might affect the straightness of the line. Recovering existing LIDAR systematic errors is not a trivial task especially that LIDAR lines are processed through the segmentation and intersection of the original LIDAR data. However, photogrammetric systematic errors can be rectified using the coplanarity constraint as shown in Equation 1 where vector V_3 in Figure 5 is explicitly expressed as a function of the sensor parameters. This explicit representation of the imaging sensor parameters can be utilized for its calibration within the bundle adjustment procedure (i.e., bundle adjustment with self-calibration). In general, the presence of uncompensated systematic errors, either in the photogrammetric or LIDAR data, will show as a poor quality of fit between the involved datasets following the registration procedure.

So far, we have addressed the three basic components of the registration methodology using straight line segments. In the next section, the same components will be discussed while using LIDAR patches as the source of control for the photogrammetric bundle adjustment.

4. Registration Methodology Using Areal Features

The previous section discussed the inclusion of straight-line features extracted from photogrammetric and LIDAR datasets in an integrated bundle adjustment procedure. LIDAR features were the source of control for the photogrammetric reconstruction. Still, such implementation required preliminary processing of LIDAR data in the form of planar patch detection and intersection. To reduce the amount of processing and avoid probable quality risks of segmenting and intersection LIDAR data, a second approach utilizing raw LIDAR point patches is presented. This approach incorporates LIDAR planar patches directly into the photogrammetric triangulation, Figure 7. The LIDAR patches are manually identified and are represented by the raw points as collected by the scanner. The only processing applied in this case is a mere blunder detection to exclude points that do not belong to the real planar surface. This processing trend targets the superiority of LIDAR in efficiently describing homogenous surfaces. The main goal sought from this implementation is to use raw LIDAR footprints, which is assumed to be free of systematic errors, as the source of control for image geo-referencing.

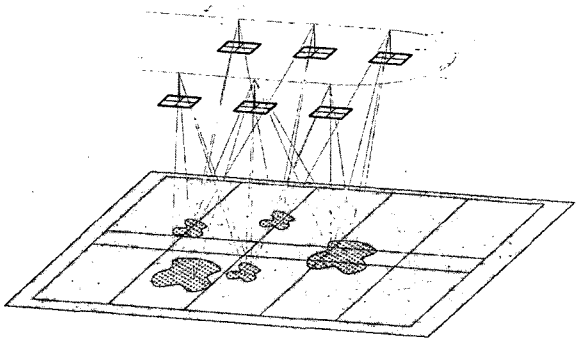

Fig. 7. LIDAR patches as a source of control for imagery.

This methodology uses identified photogrammetric patches and the points of the conjugate patch from LIDAR data. It is important to stress the following points:

- No point correspondence is required between the LIDAR and photogrammetric patches,
- Raw LIDAR points will be used after the preliminary processing for the purpose of blunder detection only, and
- The correspondence and matching between the photogrammetric and LIDAR patches is achieved manually.

4.1 Photogrammetric and LIDAR Planar Patches

The algorithm will mainly focus, similar to the case of straight-line features, on the characteristics of planar patches in both datasets. Let us consider, for example, an urban area that is rich with well-defined planar patches, where photogrammetric and LIDAR coverage is available, Figure 8 (a). The photogrammetric planar surface will be identified and represented by three points, Figure 8 (b), which is the minimum number of points required to explicitly define a plane. On the other hand, LIDAR planar patches, which are conjugate

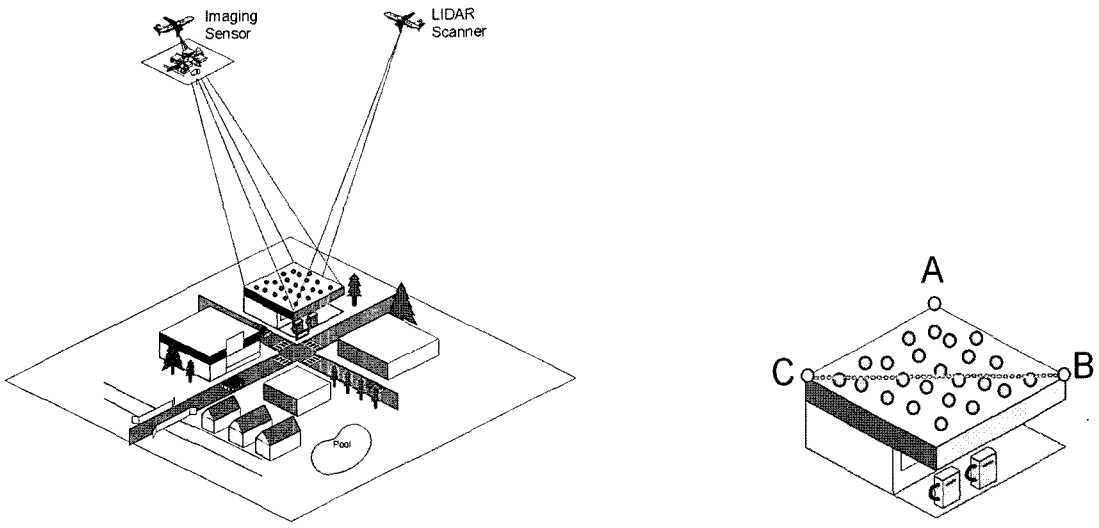

Fig. 8. Photogrammetric and LIDAR coverage of a common planar surface (a), and the minimum number of points (A,B,C) to identify a planar patch in an image (b).

to that identified in the photogrammetric dataset, are manually located. LIDAR points are grouped and labeled, then filtered for blunders and outliers with no further segmentation or feature extraction processing.

4.2 Transformation Function and Similarity Measure

The core principle behind this methodology is that in the absence of systematic errors, LIDAR points belonging to a certain planar-surface patch should coincide with the photogrammetric patch representing the same object space surface, Figure 9.

Let us consider a surface patch that is represented by two sets of points, Figure 10, namely the photogrammetric $S_P=\{A, B, C\}$ set and the LIDAR $S_L=\{(X_i, Y_i, Z_i), i=1 \text{ to } n\}$ set. Since the LIDAR points are randomly distributed, no point-to-point correspondences can be assumed between the datasets; nevertheless, all points are coplanar. For the point (X_i, Y_i, Z_i) from the LIDAR set to correspond to the same planar patch represented by the three photogrammetric points A, B, and C, it must satisfy the coplanarity constraint shown in Equation 2.

$$\begin{vmatrix} X_i & Y_i & Z_i & 1 \\ X_A & Y_A & Z_A & 1 \\ X_B & Y_B & Z_B & 1 \\ X_C & Y_C & Z_C & 1 \end{vmatrix} = \begin{vmatrix} X_i - X_A & Y_i - Y_A & Z_i - Z_A \\ X_B - X_A & Y_B - Y_A & Z_B - Z_A \\ X_C - X_A & Y_C - Y_A & Z_C - Z_A \end{vmatrix} \quad (2)$$

The above constraint is used as the basis for incorporating LIDAR points into the photogrammetric triangulation. In physical terms, this constraint means that the normal distance between any LIDAR point and the photogrammetric surface should be zero, or the volume of the tetrahedron comprised of the four

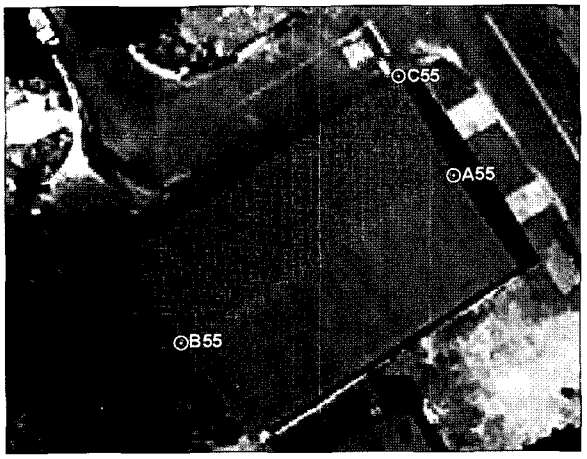

Fig. 9. Photogrammetric (A,B,C points) and LIDAR surface patches.

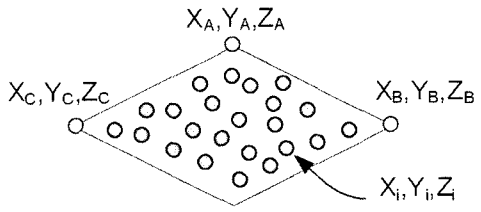

○ Photogrammetric Surface Points ○ LIDAR Points

Fig. 10. Photogrammetric and LIDAR points.

points is also equal to zero when these points are coplanar. The ground coordinates of points A, B, and C, which are unknown at the beginning, are related to their image coordinates through the collinearity equations. This constraint is applied for all LIDAR points that are part of this surface patch. The same procedure is applied again for another candidate patch and so on.

Another advantage of this approach can be noticed when considering the systematic errors of a LIDAR system. If the system model is available with explicit expression of the errors terms, the raw LIDAR points (X_i Y_i Z_i) in Equation 2 can be replace by the LIDAR equation. In this case, any unknown error terms can be solved for in the overall bundle adjustment procedure.

After addressing the three basic components of the registration methodology using straight-line segments and areal patches, the performance of these components will be evaluated in the experimental result section using simulated and real data that have been captured by a professional analog camera and a high end LIDAR system.

5. Experimental Work and Results

To examine the feasibility of using straight-line segments and planar patches for the co-registration of LIDAR and photogrammetric data, a set of experiments is designed and implemented. Within the conducted experiments, the performance will be judged by check point analysis. Furthermore, prior research (Habib 2002a) has demonstrated the feasibility of using linear features in a self-calibrating bundle adjustment. Hence, only planar patches are tested for their usability in a self-calibration procedure.

5.1 Involved Datasets

A photogrammetric and LIDAR datasets are involved in this study. Table 1 summarizes the properties of the photogrammetric dataset (scanned analog images captured by a metric analog camera - RC-10). The table also shows expected horizontal and vertical accuracies considering the pixel size, image coordinate measurement accuracy, image scale, and height-base ratio. The LIDAR dataset was captured using an OPTECH ALTM 2050 laser scanner with an average flying height of 975 m and mean point density of 2.24 points/m^2 ($\sim$0.7 m point spacing). The range and intensity data were recorded. According to the sensor and flight specifications, 0.5 m horizontal and 0.15 m vertical accuracies are expected.

Table 1. Specifications of the photogrammetric datasets.

Camera model	RC10 Real
Focal length (mm)	153.167
Frame size (W x H)	9" x 9"
# of captured images	7
# of control points surveyed	31
Avg. flying height (m)	1375
Avg. base (m)	700
Pixel size (mm)	0.024
Expected image measurement accuracy (mm)	± 0.024
Expected accuracy (assuming one pixel measurement error)	
planimetric (m)	0.21
vertical (m)	0.60

5.2 Results

In order to have a reference against which to validate the results obtained using LIDAR control lines and control patches, a point-based bundle adjustment is performed without incorporating any of the LIDAR lines or patches. To do this, a set of tie and pre-surveyed points were identified and measured in the imagery. A part of the pre-surveyed points was allocated to be used for control while the rest were used as check points. The check point analysis for this run is shown in Table 2. The line-based and the patch-based bundle adjustments are then conducted using LIDAR lines or patches as the only source of control leaving all pre-surveyed points as check points.

5.2.1 Linear Features

One hundred and nine lines were extracted from the LIDAR data and used as control for the bundle adjustment procedure. Table 3 summarizes the quality of the aligned photogrammetric dataset through check point analysis. The second column shows the results from using the same 24 check points used to analyze the results from the point-controlled bundle adjustment, while the third column shows the results when all 31

Table 2. Check points analysis for point-controlled bundle adjustment.

Control points used: 11			
	24 check points		
	Mean error, m	Std Dev, m	RMSE, m
X	0.064542	0.268651	0.276295
Y	-0.052500	0.167505	0.175540
Z	0.136975	0.203968	0.245693

Table 3. Check points analysis for LIDAR line-controlled bundle adjustment.

Control lines used: 109						
	24 check points			31 check points		
	Mean error	Std Dev	RMSE	Mean error	Std Dev	RMSE
X	-0.036333	0.283205	0.285526	-0.049581	0.252595	0.257415
Y	-0.110833	0.165749	0.199391	-0.097161	0.156840	0.184497
Z	0.189198	0.292658	0.348489	0.137747	0.309659	0.338915

available check points were used for analysis. When compared to Table 2, the results presented in Table 3 demonstrate the feasibility of using control LIDAR lines in the photogrammetric bundle adjustment.

5.2.2 Planar Patches

To monitor the performance of the patch-controlled bundle adjustment, a simulated dataset comprised of a stereopair with 60% overlap was generated using RC10 camera parameters over a simulated terrain of ±50 meters elevation variation. Eighty two control points were available in the overlap area. For the LIDAR data, 36 patches were generated parallel to the principal planes of the coordinate system (XY, XZ, and YZ).

Simulated Datasets

The first experiment was conducted using nine of the ground control points as the sole source control, the remaining 73 points were left to be used as check points. Table 4 shows the RMS error analysis of

Table 4. Check points analysis for point-controlled bundle adjustment of the simulated data.

Control points used: 9			
	73 check points		
	Mean error	Std Dev	RMSE
X	-0.051155	0.133895	0.143334
Y	0.021172	0.125091	0.126870
Z	0.055013	0.178976	0.187240

Table 5. Check points analysis for patch-controlled bundle adjustment of the simulated data

Control patches used: 36			
	73 check points		
	Mean error	Std Dev	RMSE
X	-0.027705	0.120442	0.123587
Y	-0.014999	0.121352	0.122276
Z	-0.006611	0.178555	0.178677

check point results from this point-controlled bundle adjustment.

The attention is now shifted to using LIDAR patches as the only source of control for the bundle adjustment, Table 5. All available control points are now used as check points. As seen in Table 5 for the RMSE analysis of check points, a complete compatibility of the results is obtained indicating the suitability of LIDAR patches in controlling the photogrammetric bundle adjustment.

In the next experiment, the findings using simulated data are to be verified using real data available for this purpose.

Real Datasets

Seventeen patches along the roof tops of residential houses were collected throughout the available images. Conjugate LIDAR patches were manually identified and segmented to be used as the source of control for the photogrammetric bundle adjustment. Table 6 summarizes the quality of the aligned photogrammetric dataset through check point analysis. The results presented in Table 6 demonstrate comparative feasibility of using control LIDAR patches to that when using control points in the photogrammetric bundle adjustment (compare Tables 2 and 6). In a closer look, the mean error columns in Table 6 shows some elevated values in the X and Y directions, which hints to the presence of slight biases in these directions. Pursuing this unexpected finding, one control point was added to the bundle adjustment in addition to the original 17 control patches, Table 7. Inspecting Table 7 for the new RMSE analysis, one can notice the disappearance of such biases. The conclusion which can be drawn from these results is that the roof tops, which are mainly closer to the horizontal direction, did not adequately constrain the reconstructed object space in the horizontal direction. The elimination of the problem using only one control point supports the efficiency in using planar patches as the source control of the bundle adjustment procedure.

Table 6. Check points analysis for patch-controlled bundle adjustment of real data.

Control patches used: 17						
	24 check points			31 check points		
	Mean error	Std Dev	RMSE	Mean error	Std Dev	RMSE
X	0.142417	0.257941	0.294645	0.145194	0.266844	0.303788
Y	0.217917	0.207978	0.301235	0.227032	0.232139	0.324703
Z	0.187974	0.210111	0.281924	0.141849	0.225675	0.266553

Table 7. Check points analysis for point and patch-controlled bundle adjustment of real data.

Control points used: 1 Control patches used: 17						
	24 check points			31 check points		
	Mean error	Std Dev	RMSE	Mean error	Std Dev	RMSE
X	0.044333	0.248262	0.252190	0.042871	0.247313	0.251001
Y	-0.025417	0.191418	0.193098	-0.017161	0.208147	0.208853
Z	0.172130	0.214102	0.274715	0.116173	0.229521	0.257247

5.2.3 Self-Calibration Using Planar Patches

Besides the use of LIDAR patches in controlling the photogrammetric bundle adjustment, further experiments were conducted to determine if such methodology can be utilized for self-calibrating the implemented camera. For analysis purposes, the estimated sensor parameters from a patch-controlled bundle adjustment with self-calibration procedure are used to perform a point-controlled bundle adjustment from which the results of check point analysis are compared to that using the original camera parameters.

Simulated Datasets

Thirty-six patches are used in a patch-controlled bundle adjustment with self-calibration of the simulated data. The estimated and original sensor (i.e., those provided in the Camera Calibration Certificate - CCC) parameters are then used in a point-controlled bundle adjustment. The check point analysis for these experiments is shown in Table 8. Comparing the results in Table 8, one can see a perfect compatibility between the reconstructed object space from the original parameters and that from the estimated ones using planar patches. Thus, LIDAR patches can be effectively used for patch-controlled bundle adjustment with self-calibration procedure.

Real Datasets

Similar to the simulated data experiments, real datasets are used to evaluate the feasibility of using LIDAR patches in a bundle adjustment with self-calibration of the implemented camera. Table 9 shows the results of these experiments, where the reconstructed object space while using the original sensor parameters in the CCC is compared to that derived while using the sensor parameters estimated from a patch-based bundle adjustment with self-calibration. Inspecting the RMSE results in Table 9, one can notice lower quality of the reconstructed object space using the estimated sensor parameters from the patch-based self-calibration procedure. In a following experiment, 10 control points were added to the patch-based self-calibration run. The results, as indicated in the second part of Table 9, show excellent compatibility

Table 8. Check points analysis for 9 point-controlled bundle adjustment using the original sensor parameters in the Camera Calibration Certificate (CCC) and patch-based self-calibration results.

	Original CCC			Calibration from 36 patches		
	Mean Error	Std Dev	RMSE	Mean Error	Std Dev	RMSE
X	-0.042719	0.117960	0.125457	-0.049231	0.119012	0.128792
Y	0.032316	0.111192	0.115792	0.035512	0.112939	0.118390
Z	0.062087	0.143207	0.156087	0.064894	0.140502	0.154765

Table 9. Check points analysis for 10 point-controlled BA using self-calibration results.

	Original CCC			Calibration from 17 Patches		
	Mean Error	Std Dev	RMSE	Mean Error	Std Dev	RMSE
X	0.064542	0.268651	0.276295	-0.000917	0.547581	0.547582
Y	-0.052500	0.167505	0.175540	-0.282917	0.592762	0.656817
Z	0.136975	0.203968	0.245693	-0.360349	0.588576	0.690126
	Original CCC			Calibration from 10 Points & 17 Patches		
	Mean Error	Std Dev	RMSE	Mean Error	Std Dev	RMSE
X	0.064542	0.268651	0.276295	0.063542	0.273262	0.280553
Y	-0.052500	0.167505	0.175540	-0.058333	0.166577	0.176496
Z	0.136975	0.203968	0.245693	0.091158	0.183032	0.204476

between the two sets of sensor parameters. Hence, the same conclusion of the inadequacy of the orientation of the measured patches can be drawn for the self-calibration case as well.

6. Conclusions and Future Work

This paper presented a comprehensive registration methodology for the alignment of LIDAR and photogrammetric models relative to a common reference frame using straight-line and areal features. The straight-line segments as well as planar patches demonstrated reliable results and feasible implementation scope. The mathematical models and the similarity measures proved to be suitable and adequate for the purposes set. These models assume the absence of biases, which cannot be modeled by rigid-body transformation, between the LIDAR and photogrammetric datasets. In addition, planar patches were proved to be suitable for implementing self-calibration procedure. To test the feasibility of the developed methodologies, we conducted several experiments using simulated and real data captured by an analog professional camera (RC-10) and a high end LIDAR system (OPTECH ALTM 2050). The outcome from these experiments suggests the following:

- Straight-line features and planar patches proved to be suitable in establishing a common reference frame for the LIDAR and photogrammetric surfaces.
- LIDAR planar patches can be utilized for self-calibrating involved cameras, provided that adequate number of patches is involved and oriented along the three principle planes of the coordinate system.

Future research work will focus on applying the planar patch approach on medium-format/low-cost digital cameras as well as line cameras. In addition, we will address the automation of the extraction of linear and planar features from photogrammetric and LIDAR data together with the correspondence between conjugate features. Also, we will be looking at the possibility of developing new visualization tools for an easier portrayal of the registration outcome. Finally, registered multi-temporal datasets will be inspected for the possibility of developing automatic change detection techniques.

Acknowledgment

We would like to thank the Korean Electronics and Telecommunication Research Institute (ETRI) for its financial support of this research. The authors are also indebted to the Technology Institute for Development (LACTEC), UFPR, Brazil for providing the LIDAR data.

References

1. Baltsavias, E. (1999). A comparison between photogrammetry and laser scanning. ISPRS Journal of Photogrammetry & Remote Sensing, 54(1):83-94.
2. Brown, L. (1992). A survey of image registration techniques, ACM Computing Surveys 24(4):325-376.
3. Ebner, H. and T. Ohlhof (1994). Utilization of ground control points for image orientation without point identification in image space. In The International Archives of Photogrammetry and Remote Sensing and Spatial Information Sciences, 30(3/1):206-211.
4. Habib, A. and T. Schenk (1999). New approach for matching surfaces from laser scanners and optical sensors, The International Archives of Photogrammetry and Remote Sensing and Spatial Information Sciences, 32(3W14):55-61.

5. Habib, A., Y. Lee and M. Morgan (2001). Surface matching and change detection using the modified Hough transform for robust parameter estimation. Photogrammetric Record Journal, 17(98):303-315.
6. Habib, A., Y. Lee and M. Morgan (2002a). Bundle adjustment with self-calibration using straight lines. Photogrammetric Record Journal, 17(100):635-650.
7. Habib, A., S. Shin and M. Morgan (2002b). New approach for calibrating off-the-shelf digital cameras. In ISPRS Commission III Symposium "Photogrammetric Computer Vision", Graz, Austria, September 9-13, 2002.
8. Kilian, J., N. Haala and M. Englich (1996). Capture and evaluation of airborne laser scanner data. In The International Archives of Photogrammetry and Remote Sensing and Spatial Information Sciences, 31(B3):383-388.
9. Kraus, K. (1993). Photogrammetry, Volume 1: Fundamentals and standard processes, Ferd. Dummler's Verlag, Bonn.
10. Lichti, D.D., Stewart, M.P., Tsakiri, M. and Snow, A.J. (2000). Benchmark tests on a three-dimensional laser scanning system. Geomatics Research Australia 72:1-23
11. Mikhail, E., J. Bethel and J. McGlone (2001). Introduction to modern photogrammetry. John Wiley & Sons, New York.
12. Postolov, Y., A. Krupnik and K. McIntosh (1999). Registration of airborne laser data to surfaces generated by photogrammetric means. In The International Archives of Photogrammetry and Remote Sensing and Spatial Information Sciences, 32(3W14):95-99.
13. Satale, D. and M. Kulkarni (2003). LiDAR in mapping. Map India Conference GISdevelopment.net. http://www.gisdevelopment.net/technology/gis/mi03129.htm (Last accessed February 14, 2005).
14. Schenk, T. (1999). Determining transformation parameters between surfaces without identical points, Technical Report Photogrammetry No. 15, Department of Civil and Environmental Engineering and Geodetic Science, OSU, 22 pages.
15. Schenk, T., S. Seo and B. Csatho (2001). Accuracy Study of airborne laser scanning data with photogrammetry, In: International Archives of Photogrammetry and Remote Sensing, vol. 34 (part 3/W4), Annapolis, MD, pp. 113.
16. Schenk, T. and B. Csathó (2002). Fusion of LIDAR data and aerial imagery for a more complete surface description. In The International Archives of Photogrammetry and Remote Sensing and Spatial Information Sciences, 34(3A):310-317.
17. Wehr, A. and U. Lohr (1999). Airborne laser scanning-an introduction and overview, ISPRS Journal Of Photogrammetry And Remote Sensing (54)2-3, pp. 68-82.